J|A|C|S
ARTICLES
Published on Web 12/13/2002

# Organometallic Complexes for Nonlinear Optics. 30.[1] Electrochromic Linear and Nonlinear Optical Properties of Alkynylbis(diphosphine)ruthenium Complexes

Clem E. Powell,[†] Marie P. Cifuentes,[†] Joseph P. Morrall,[†] Robert Stranger,[†] Mark G. Humphrey,*[,†] Marek Samoc,[‡] Barry Luther-Davies,[‡] and Graham A. Heath[§]

*Contribution from the Department of Chemistry, Australian National University, Canberra ACT 0200, Australia, Australian Photonics Cooperative Research Centre, Laser Physics Centre, Research School of Physical Sciences and Engineering, Australian National University, Canberra ACT 0200, Australia, and Research School of Chemistry, Australian National University, Canberra ACT 0200, Australia*

Received July 15, 2002; E-mail: Mark.Humphrey@anu.edu.au

***Abstract:*** A combination of cyclic voltammetry, UV−vis−NIR spectroelectrochemistry, time-dependent density functional theory (TD-DFT), and *Z*-scan measurements employing a modified optically transparent thin-layer electrochemical (OTTLE) cell has been used to identify and assign intense transitions of metal alkynyl complexes at technologically important wavelengths in the oxidized state and to utilize these transitions to demonstrate a facile electrochromic switching of optical nonlinearity. Cyclic voltammetric data for the ruthenium(II) complexes *trans*-[RuXY(dppe)$_2$] [dppe = 1,2-bis(diphenylphosphino)ethane, X = Cl, Y = Cl (**1**), C≡CPh (**2**), 4-C≡CC$_6$H$_4$C≡CPh (**3**); X = C≡CPh, Y = C≡CPh (**4**), 4-C≡CC$_6$H$_4$C≡CPh (**5**)] show a quasi-reversible oxidation at 0.50−0.60 V (with respect to ferrocene/ferrocenium 0.56 V), which is assigned to the Ru$^{II/III}$ couple. The ruthenium(III) complex cations *trans*-[RuXY(dppe)$_2$]$^+$ were obtained by the in situ oxidation of complexes **1**−**5** using an OTTLE cell. The UV−vis−NIR optical spectra of **1**$^+$−**5**$^+$ contain a low-energy band in the near-IR region (∼8000−16 000 cm$^{-1}$), in contrast to **1**−**5**, which are optically transparent at wavelengths < 22 000 cm$^{-1}$. TD-DFT calculations have been applied to model systems *trans*-[RuXY(PH$_3$)$_4$] [X = Cl, Y = Cl, C≡CPh, or 4-C≡CC$_6$H$_4$C≡CPh; X = C≡CPh, Y = C≡CPh or 4-C≡CC$_6$H$_4$C≡CPh] to rationalize the optical spectra of **1**−**5** and **1**$^+$−**5**$^+$. The important low-energy bands in the electronic spectra of **1**$^+$−**5**$^+$ are assigned to the promotion of an electron from either a chloride p orbital or an ethynyl p orbital to the partially occupied HOMO. These absorption bands have been utilized to demonstrate a facile switching of cubic nonlinear optical (NLO) properties at 12 500 cm$^{-1}$ (corresponding to the wavelength of maximum transmission in biological materials such as tissue) using the OTTLE cell, the first electrochromic switching of molecular nonlinear refraction and absorption, and the first switching of optical nonlinearity using an electrochemical cell.

## Introduction

Alkynylmetal complexes have attracted significant attention because of their intrinsic interest,[2,3] as well as their potential applications in homogeneous and heterogeneous catalysis, nonlinear optics, the development of conducting materials, and as key components in artificial light-harvesting chromophores.[4−8] Germane to these possible applications are their electronic properties which, as a consequence, have prompted a large number of studies. Electrochemical investigations employing cyclic voltammetry have been carried out on a significant number of mononuclear alkynyl complexes, with attention focused on inter alia the nature of the metal alkynyl interaction, radical−radical coupling to afford dimeric species, and cationic complex hydrogen abstraction to afford vinylidene complexes; for recent studies in this field, see refs 9−25.

[†] Department of Chemistry, Australian National University.
[‡] Research School of Physical Sciences and Engineering, Australian National University.
[§] Research School of Chemistry, Australian National University.

(1) Part 29: Hurst, S. K.; Lucas, N. T.; Humphrey, M. G.; Isoshima, T.; Wostyn, K.; Asselberghs, I.; Clays, K.; Persoons, A.; Samoc, M.; Luther-Davies, B. *Inorg. Chim. Acta*, in press.
(2) Nast, R. *Coord. Chem. Rev.* **1982**, *47*, 89.
(3) Manna, J.; John, K. D.; Hopkins, M. D. *Adv. Organomet. Chem.* **1995**, *38*, 79.
(4) McGrady, J. E.; Lovell, T.; Stranger, R.; Humphrey, M. G. *Organometallics* **1997**, *16*, 4004.
(5) Calabrese, J. C.; Cheng, L.-T.; Green, J. C.; Marder, S. R.; Tam, W. *J. Am. Chem. Soc.* **1991**, *113*, 7227.
(6) Canadell, E.; Alvarez, S. *Inorg. Chem.* **1984**, *23*, 573.
(7) Frapper, G.; Kertesz, M. *Inorg. Chem.* **1993**, *32*, 732.
(8) Bianchini, C.; Meli, A.; Peruzzini, M.; Vacca, A.; Laschi, F.; Zanello, P.; Ottaviani, F. M. *Organometallics* **1990**, *9*, 360.
(9) Winter, R. F.; Hornung, F. M. *Organometallics* **1999**, *18*, 4005.
(10) Zhu, Y.; Millet, D. B.; Wolf, M. O.; Rettig, S. J. *Organometallics* **1999**, *18*, 1930.
(11) Choi, M.-Y.; Chan, M. C.-W.; Zhang, S.; Cheung, K.-K.; Che, C.-M.; Wong, K.-Y. *Organometallics* **1999**, *18*, 2074.
(12) Denis, R.; Toupet, L.; Paul, F.; Lapinte, C. *Organometallics* **2000**, *19*, 4240.
(13) Touchard, D.; Haquette, P.; Daridor, A.; Romero, A.; Dixneuf, P. H. *Organometallics* **1998**, *17*, 3844.
(14) Back, S.; Gossage, R. A.; Lutz, M.; del Rio, I.; Spek, A. L.; Lang, H.; van Koten, G. *Organometallics* **2000**, *19*, 3296.

 **10.1021/ja0277125 CCC: $25.00** 

The desire to rationalize the electronic properties of alkynylmetal complexes has prompted a large number of theoretical studies. Many reports have focused on dinuclear or polynuclear complexes in which the metal centers are connected by a range of potentially $\pi$-delocalizable bridging groups, and in which the primary objective of the study was to understand the nature of the metal−metal interaction.[26−32] Monometallic complexes have also commanded attention, primarily because of the lingering uncertainty about the nature of the metal−alkynyl bonding interaction and, in particular, the existence or otherwise of a $\pi$-back-bonding component.[4,21,33−46]

A current major focus of alkynylmetal research is their possible application in nonlinear optics. New materials with desirable nonlinear optical (NLO) properties are expected to provide an efficient means of controlling and processing light beams used in photonic technologies;[47] to this end, the NLO properties of a vast panoply of organic, inorganic, and organometallic compounds have been studied. While there has been considerable success in the past decade at preparing compounds with large intrinsic nonlinearities, attention has recently focused on possibilities for reversibly modulating ("switching") nonlinearities.[48] This is an area of NLO materials research in which inorganic molecular materials may be superior to organics. Inorganic complexes can potentially have their NLO properties switched by a variety of methods. They should be easier to switch magnetically than organic molecules,[49] although this has yet to be demonstrated. The metal coordination of Schiff bases switches on quadratic nonlinearity,[50−52] but this is not reversible. The switching of quadratic and cubic nonlinearities by protonation/deprotonation chemistry has been demonstrated with some ruthenium complexes,[19] but this procedure is probably only of academic interest and little practical utility. Of relevance to the present studies, chemical oxidation and subsequent reduction of specific iron and ruthenium complexes have been employed to switch molecular first hyperpolarizability;[53,54] however, chemical oxidation and reduction remote from the optical bench, coupled to dilution requirements before measurement, rendered this a less-than-ideal approach to switching nonlinearity.

Alkynylmetal complexes can have significant NLO properties and easily accessible oxidation states,[16−20,47,55−68] a combination


(15) Naulty, R. H.; McDonagh, A. M.; Whittall, I. R.; Cifuentes, M. P.; Humphrey, M. G.; Houbrechts, S.; Maes, J.; Persoons, A.; Heath, G. A.; Hockless, D. C. R. *J. Organomet. Chem*. **1998**, *563*, 137.
(16) McDonagh, A. M.; Cifuentes, M. P.; Lucas, N. T.; Humphrey, M. G.; Houbrechts, S.; Persoons, A. *J. Organomet. Chem*. **2000**, *205*, 193.
(17) McDonagh, A. M.; Lucas, N. T.; Cifuentes, M. P.; Humphrey, M. G.; Houbrechts, S.; Persoons, A. *J. Organomet. Chem*. **2000**, *605*, 184.
(18) McDonagh, A. M.; Cifuentes, M. P.; Humphrey, M. G.; Houbrechts, S.; Maes, J.; Persoons, A.; Samoc, M.; Luther-Davies, B. *J. Organomet. Chem.* **2000**, *610*, 71.
(19) Hurst, S.; Cifuentes, M. P.; Morrall, J. P. L.; Lucas, N. T.; Whittall, I. R.; Humphrey, M. G.; Asselberghs, I.; Persoons, A.; Samoc, M.; Luther-Davies, B.; Willis, A. C. *Organometallics* **2001**, *20*, 4664.
(20) Hurst, S.; Lucas, N. T.; Cifuentes, M. P.; Humphrey, M. G.; Samoc, M.; Luther-Davies, B.; Asselberghs, I.; Van Boxel, R.; Persoons, A. *J. Organomet. Chem*. **2001**, *633*, 114.
(21) Adams, C. J.; James, S. L.; Lin, X.; Raithby, P. R.; Yellowlees, L. J. *J. Chem. Soc., Dalton Trans.* **2000**, 63.
(22) Yam, V. W.-W.; Tang, R. P.-L.; Wong, K. M.-C.; Cheung, K.-K. *Organometallics* **2001**, *20*, 4476.
(23) McGarrah, J. E.; Kim, Y.-J.; Hissler, M.; Eisenberg, R. *Inorg. Chem.* **2001**, *40*, 4510.
(24) McAdam, C. J.; Blackie, E. J.; Morgan, J. L.; Mole, S. A.; Robinson, B. H.; Simpson, J. *J. Chem. Soc., Dalton Trans.* **2001**, 2362.
(25) Fillaut, J.-L.; Price, M.; Johnson, A. L.; Perruchon, J. *J. Chem. Soc., Chem. Commun.* **2001**, 739.
(26) Beljonne, D.; Colbert, M. C. B.; Raithby, P. R.; Friend, R. H.; Brédas, J. L. *Synth. Met.* **1996**, *81*, 179.
(27) Weyland, T.; Lapinte, C.; Frapper, G.; Calhorda, M. J.; Halet, J.-F.; Toupet, L. *Organometallics* **1997**, *16*, 2024.
(28) Long, N. J.; Martin, A. J.; Vilar, R.; White, A. J. P.; Williams, D. H.; Younus, M. *Organometallics* **1999**, *18*, 4261.
(29) Colbert, M. C. B.; Lewis, J.; Long, N. J.; Raithby, P. R.; Younus, M.; White, A. J. P.; Williams, D. J.; Payne, N. N.; Yellowlees, L.; Beljonne, D.; Chawdhury, N.; Friend, R. H. *Organometallics* **1998**, *17*, 3034.
(30) Belanzoni, P.; Re, N.; Sgamellotti, A.; Floriani, C. *J. Chem. Soc., Dalton Trans.* **1997**, 4773.
(31) Unseld, D.; Krivykh, V. V.; Heinze, K.; Wild, F.; Artus, G.; Schmalle, H.; Berke, H. *Organometallics* **1999**, *18*, 1525.
(32) Low, P. J.; Rousseau, R.; Lam, P.; Udachin, K. A.; Enright, G. D.; Tse, J. S.; Wayner, D. D. M.; Carter, A. J. *Organometallics* **1999**, *18*, 3885.
(33) De Angelis, F.; Re, N.; Rosi, M.; Sgamellotti, A.; Floriani, C. *J. Chem. Soc., Dalton Trans.* **1997**, 3841.
(34) Peréz-Carreño, E.; Paoli, P.; Ienco, A.; Mealli, C. *Eur. J. Inorg. Chem.* **1999**, 1315.
(35) Knight, E. T.; Myers, L. K.; Thompson, M. E. *Organometallics* **1992**, *11*, 3691.
(36) Louwen, J. N.; Hengelmolen, R.; Grove, D. M.; Oskam, A. *Organometallics* **1984**, *3*, 908.
(37) Ara, I.; Berengure, J. R.; EguizEabal, E.; Forniés, J.; Gómez, J.; Lalinde, E.; Sáez-Rocher, J. M. *Organometallics* **2000**, *19*, 4385.
(38) Lichtenberger, D. L.; Renshaw, S. K.; Bullock, R. M. *J. Am. Chem. Soc*. **1993**, *115*, 3276.
(39) Khan, M. S.; Kakkar, A. K.; Ingham, S. L.; Raithby, P. R.; Lewis, J.; Spencer, B.; Wittmann, F.; Friend, R. H. *J. Organomet. Chem*. **1994**, *472*, 247.
(40) Whittall, I. R.; Humphrey, M. G.; Hockless, D. C. R.; Skelton, B. W.; White, A. H. *Organometallics* **1995**, *14*, 3970.
(41) Whittall, I. R.; Humphrey, M. G.; Persoons, A.; Houbrechts, S. *Organometallics* **1996**, *15*, 1935.
(42) Whittall, I. R.; Cifuentes, M. P.; Humphrey, M. G.; Luther-Davies, B.; Samoc, M.; Houbrechts, S.; Persoons, A.; Heath, G. A.; Hockless, D. C. R. *J. Organomet. Chem*. **1997**, *549*, 127.
(43) Rourke, J. P.; Stringer, G.; Chow, P.; Deeth, R. J.; Yufit, D. M.; Howard, J. A. K.; Marder, T. B. *Organometallics* **2002**, *21*, 429.
(44) Klein, A.; Slageren, J. v.; Zâlis, S. *J. Organomet. Chem*. **2001**, *620*, 202.
(45) Jagadeesh, M. N.; Thiel, W.; Köhler, J.; Fehn, A. *Organometallics* **2002**, *21*, 2076.
(46) Delfs, C. D.; Stranger, R.; Humphrey, M. G.; McDonagh, A. M. *J. Organomet. Chem*. **2000**, *607*, 208.
(47) Cifuentes, M. P.; Powell, C. E.; Humphrey, M. G.; Heath, G. A.; Samoc, M.; Luther-Davies, B. *J. Phys. Chem. A* **2001**, *105*, 9625.
(48) Coe, B. J. *Chem.−Eur. J.* **1999**, *5*, 2464.
(49) Gaudry, J.-B.; Capes, L.; Langot, P.; Marcen, S.; Kollmannsberger, M.; Freysz, E.; Letard, J. F.; Kahn, O. *Chem. Phys. Lett.* **2000**, *324*, 321.
(50) Di Bella, S.; Fragalà, I.; Ledoux, I.; Diaz-Garcia, M. A.; Marks, T. *J. Chem. Mater*. **1994**, *6*, 881.
(51) Di Bella, S.; Fragalà, I.; Ledoux, I.; Diaz-Garcia, M. A.; Marks, T. J. *J. Am. Chem. Soc*. **1997**, *119*, 9550.
(52) Di Bella, S.; Fragalà, I. *Synth. Met*. **2000**, *115*, 191.
(53) Coe, B. J.; Houbrechts, S.; Asselberghs, I.; Persoons, A. *Angew. Chem., Int. Ed.* **1999**, *38*, 366.
(54) Malaun, M.; Reeves, Z. R.; Paul, R. L.; Jeffery, J. C.; McCleverty, J. A.; Ward, M. D.; Asselberghs, I.; Clays, K.; Persoons, A. *Chem. Commun*. **2001**, 49.
(55) McDonagh, A. M.; Humphrey, M. G.; Samoc, M.; Luther-Davies, B.; Houbrechts, S.; Wada, T.; Sasabe, H.; Persoons, A. *J. Am. Chem. Soc*. **1999**, *121*, 1405.
(56) McDonagh, A. M.; Humphrey, M. G.; Samoc, M.; Luther-Davies, B. *Organometallics* **1999**, *18*, 5195.
(57) Cifuentes, M. P.; Driver, J.; Humphrey, M. G.; Asselberghs, I.; Persoons, A.; Samoc, M.; Luther-Davies, B. *J. Organomet. Chem*. **2000**, *607*, 72.
(58) Houbrechts, S.; Wada, T.; Sasabe, H.; Morrall, J. P. L.; Whittall, I. R.; McDonagh, A. M.; Humphrey, M. G.; Persoons, A. *MCLC S&T, Sect. B: Nonlinear Opt.* **1999**, *22*, 165.
(59) Weyland, T.; Ledoux, I.; Brasselet, S.; Zyss, J.; Lapinte, C. *Organometallics* **2000**, *19*, 5235.
(60) Casalboni, M.; Sarcinelli, F.; Pizzoferrato, R.; D′Amato, R.; Furlani, A.; Russo, M. V. *Chem. Phys. Lett.* **2000**, *319*, 107.
(61) Vicente, J.; Chicote, M. T.; Abrisqueta, M. D.; Ramîrez de Arellano, M. C.; Jones, P. G.; Humphrey, M. G.; Cifuentes, M. P.; Samoc, M.; Luther-Davies, B. *Organometallics* **2000**, *19*, 2968.
(62) Samoc, M.; Humphrey, M. G.; Cifuentes, M. P.; McDonagh, A. M.; Powell, C. E.; Heath, G. A.; Luther-Davies, B. *SPIE Proc.−Int. Soc. Opt. Eng.* **2001**, *4461*, 65.
(63) Siemsen, P.; Gubler, U.; Bosshard, C.; Günter, P.; Diederich, F. *Chem.−Eur. J.* **2001**, *7*, 1333.
(64) Hurst, S. K.; Cifuentes, M. P.; McDonagh, A. M.; Humphrey, M. G.; Samoc, M.; Luther-Davies, B.; Asselberghs, I.; Persoons, A. *J. Organomet. Chem*. **2002**, *642*, 259.
(65) Hurst, S. K.; Lucas, N. T.; Humphrey, M. G.; Asselberghs, I.; Van Boxel, R.; Persoons, A. *Aust. J. Chem.* **2001**, *54*, 447.
(66) Garcia, M. H.; Rabalo, M. P.; Dias, A. R.; Duarte, M. T.; Wenseleers, W.; Aerts, G.; Goovaerts, E.; Cifuentes, M. P.; Hurst, S.; Humphrey, M. G.; Samoc, M.; Luther-Davies, B. *Organometallics* **2002**, *21*, 2107.
(67) D'Amato, R.; Furlani, A.; Colapietro, M.; Portalone, G.; Casalboni, M.; Falconieri, M.; Russo, M. V. *J. Organomet. Chem*. **2001**, *627*, 13.
(68) Cadierno, V.; Conejero, S.; Gamasa, M. P.; Gimeno, J.; Asselberghs, I.; Houbrechts, S.; Clays, K.; Persoons, A.; Borge, J.; Garciá-Granda, S. *Organometallics* **1999**, *18*, 582.

suggestive of a potential for NLO switching. We present herein cyclic voltammetric and UV−vis−NIR spectroelectrochemical studies on the systematically varied series of complexes *trans*-[RuXY(dppe)$_2$] [dppe = 1,2-bis(diphenylphosphino)ethane, X = Cl, Y = Cl (**1**), C≡CPh (**2**), or 4-C≡CC$_6$H$_4$C≡CPh (**3**); X = C≡CPh, Y = C≡CPh (**4**) or 4-C≡CC$_6$H$_4$C≡CPh (**5**)], together with TD-DFT calculations on the model systems *trans*-[RuXY(PH$_3$)$_4$] [X = Cl, Y = Cl, C≡CPh, 4-C≡CC$_6$H$_4$C≡CPh; X = C≡CPh, Y = C≡CPh, 4-C≡CC$_6$H$_4$C≡CPh], the latter rationalizing the unique spectral properties of the title complexes. We also report facile cubic NLO switching using the low-energy optical transitions for the oxidized forms of **3**, **5**, and the related complex *trans*-[Ru(C≡CPh)Cl(dppm)$_2$] (**6**) by utilizing an optically transparent thin-layer electrochemical (OTTLE) cell, in a general procedure which could also be employed to switch quadratic nonlinearities. This is the first electrochromic switching of molecular nonlinear refraction and absorption. This phenomenon is demonstrated at 800 nm, the wavelength at which biological materials such as tissue have maximum transparency, suggesting possible applications in medical imaging. Our preliminary switching results for **3** at 800 nm have been briefly communicated.[47]

## Experimental Section

**Synthetic Procedures.** The complexes *trans*-[Ru(C≡CPh)Cl(dppm)$_2$] (**6**),[69] *cis*-[RuCl$_2$(dppe)$_2$] and *trans*-[RuXY(dppe)$_2$] [X = Cl, Y = Cl (**1**),[70] C≡CPh (**2**),[71] X = C≡CPh, Y = C≡CPh (**4**),[71] 4-C≡CC$_6$H$_4$C≡CPh (**5**)[55]], and the alkyne 4-HC≡CC$_6$H$_4$C≡CPh were prepared according to literature procedures. Synthesis of *trans*-[Ru(4-C≡CC$_6$H$_4$C≡CPh)Cl(dppe)$_2$] (**3**): A mixture of *cis*-[RuCl$_2$(dppe)$_2$] (161 mg, 0.149 mmol), 4-HC≡CC$_6$H$_4$C≡CPh (41 mg, 0.203 mmol), and ammonium hexafluorophosphate (43 mg, 0.264 mmol) was stirred in dichloromethane (40 mL) for 16 h. The mixture was taken to dryness in vacuo and triturated with ether (3 × 15 mL). Dichloromethane (30 mL) and triethylamine (2 mL) were added to the residual solid, and the resultant solution was stirred for 30 s. The solution was taken to dryness in vacuo, and the residue was purified by column chromatography on alumina, eluting with 20% dichloromethane/80% petrol to remove the bis-alkynyl product (trace quantities) and then with acetone to remove the product. The product was recrystallized by the liquid diffusion of methanol into a dichloromethane solution to afford orange crystals of *trans*-[Ru(4-C≡CC$_6$H$_4$C≡CPh)Cl(dppe)$_2$] (**3**) as the hemidichloromethane solvate, yield 94 mg (54%). MALDI MS: 1134 ([M]$^+$, 90), 1100 ([MH − Cl]$^+$, 90), 934 ([MH − C$_2$C$_6$H$_4$C$_2$Ph]$^+$, 95), 899 ([MH − C$_2$C$_6$H$_4$C$_2$Ph − Cl]$^+$, 100). Anal. Calcd for C$_{68}$H$_{57}$ClP$_4$Ru.0.5CH$_2$Cl$_2$: C, 69.90; H, 4.97%. Found: C, 69.74; H, 5.02%. $^1$H NMR ($\delta$, 300 MHz, CDCl$_3$): 2.67 (m, 8H, CH$_2$), 5.28 (s, 1H, CH$_2$Cl$_2$), 6.53−7.52 (m, 49H, phenyl). $^{31}$P NMR ($\delta$, 121 MHz, CDCl$_3$): 49.7 (s, PPh$_2$).

**Electrochemical and Spectroelectrochemical Studies.** Cyclic voltammetric measurements were recorded using a MacLab 400 interface and MacLab potentiostat from AD Instruments (using Pt disk working, Pt auxiliary, and Ag−AgCl reference minielectrodes from Cypress Systems). Scan rates were typically 100 mV s$^{-1}$. Electrochemical solutions contained 0.1 M (NBu$^n_4$)PF$_6$ and ∼10$^{-3}$ M complex in dichloromethane. Solutions were purged and maintained under an atmosphere of nitrogen. All values are referenced to an internal ferrocene/ferrocenium couple ($E°$ at 0.56 V). Electronic spectra (45 000−4000 cm$^{-1}$) were recorded on a Perkin-Elmer Lambda 9 spectrophotometer. Solution spectra of the oxidized species at 253 K were obtained by electrogeneration (Thompson 401E potentiostat) at a Pt gauze working electrode within a cryostatted OTTLE cell, path length 0.5 mm, mounted within the spectrophotometer.[72] The electrogeneration potential was ∼300 mV beyond $E_{1/2}$ for each couple, to ensure complete electrolysis. The efficiency and reversibility of each step was tested by applying a sufficiently negative potential to reduce the product; stable isosbestic points were observed in the spectral progressions for all the transformations reported herein.

**Computational Methods.** All calculations described in this work were performed on a Linux-based Pentium III (600 MHz) computer using the Amsterdam Density Functional (ADF) program, version 1999, developed by Baerends et al.[73−75] The local exchange correlation approximation of Vosko, Wilk, and Nusair[76] was used along with the corrections of Becke[77] and Perdew.[78] A triple-$\zeta$ basis set (type IV) was used for all atoms. Core orbitals were frozen through 1s (C), 2p (P, Cl), and 3p (Ru). Geometries were optimized using the algorithm of Versluis and Ziegler.[79] Optical excitation energies of closed shell complexes were calculated using the RESPONSE module[80] of ADF. $C_{2v}$ symmetry was used for all complexes, with a coordinate system having the *z*-axis along the metal−acetylide bond axis and the *x* axis in the plane of the phenyl rings. To reduce computational expense, each dppe ligand was replaced with two PH$_3$ ligands. Phenyl rings were constrained to be coplanar, and the PH$_3$ ligands are staggered with respect to the phenyl rings.

***Z*-Scan Studies.** Measurements were performed at 800 nm (12 500 cm$^{-1}$) using 100 fs pulses from a system consisting of a Coherent Mira titanium−sapphire laser pumped with a Coherent Verdi cw pump and a titanium−sapphire regenerative amplifier pumped with a frequency-doubled Q-switched pulsed Nd:YAG laser (Spectra Physics GCR) at 30 Hz and employing chirped pulse amplification. *Z*-scan measurements were also attempted at 1180 nm (8470 cm$^{-1}$) and 1300 nm (7690 cm$^{-1}$) using another high-power femtosecond laser system with a 775 nm titanium−sapphire regenerative amplifier (Clark-MXR CPA-2001A) pumping a Light Conversion Topas optical parametric amplifier. This system provides tunable, approximately 150 fs pulses with a repetition rate of 1 kHz. For both femtosecond systems, the energy per pulse used in the experiments was limited (using a halfwave plate/polarizer combination and/or neutral density filters) to approximately 1 $\mu$J. Argon-saturated dichloromethane solutions of **3**, **5**, and **6** containing ∼0.3 M (NBu$^n_4$)PF$_6$ supporting electrolyte were examined in an OTTLE cell (with Pt auxiliary, Pt working, and Ag−AgCl reference electrodes), path length 0.5 mm, with the laser beam passing through a focusing lens and directed along the axis passing through a 1.5 mm diameter hole in the Pt sheet working electrode. The electrochemical cell was mounted on a computer driven translation stage, as usual in *Z*-scan measurements.[81] The $w_0$ parameter of the beam (the radius at the $1/e^2$ intensity point) was chosen to be in the range 35−45 $\mu$m. The Rayleigh length $z_R = \pi w_0^2/\lambda$, where $w_0$ is the Gaussian beam waist and $\lambda$ is the wavelength, was thus taken to be $z_R > 3$ mm (which corresponds to $w_0 > 30$ $\mu$m for $\lambda = 0.8$ $\mu$m). A "thin sample" assumption was therefore considered to be justified. In effect, one can then treat the total effect of the third-order nonlinearity of all the components of the system, the solution (solvent and dissolved materials), and the glass walls of the cell as being an additive quantity. The beam "cropping" by the aperture was also negligible over the range of travel of the cell ($z = -3$ cm to

(69) Touchard, D.; Haquette, P.; Pirio, N.; Toupet, L.; Dixneuf, P. H. *Organometallics* **1993**, *12*, 3132.
(70) Chatt, J.; Hayter, R. G. *J. Chem. Soc., Dalton Trans.* **1961**, 896.
(71) Touchard, D.; Haquette, P.; Guesmi, S.; Pichon, L. L.; Daridor, A.; Toupet, L.; Dixneuf, P. H. *Organometallics* **1997**, *16*, 3640.
(72) Duff, C. M.; Heath, G. A. *Inorg. Chem.* **1991**, *30*, 2528.
(73) Baerends, E. J.; Ellis, D. E.; Ros, P. *Chem. Phys.* **1973**, *2*, 42.
(74) Baerends, E. J.; Ros, P. *Int. J. Quantum Chem.* **1978**, *s12*, 169.
(75) teVelde, G.; Baerends, E. J. *J. Comput. Phys.* **1992**, *99*, 84.
(76) Vosko, S. H.; Wilk, L.; Nusair, M. *Can. J. Phys.* **1980**, *58*, 1200.
(77) Becke, A. D. *J. Chem. Phys.* **1986**, *84*, 4524.
(78) Perdew, J. P.; Chevary, J. A.; Vosko, S. H.; Jackson, K. A.; Pederson, M. R.; Singh, D. J.; Fiolhais, C. *Phys. Rev. A.* **1992**, *46*, 6671.
(79) Versluis, L.; Ziegler, T. *J. Chem. Phys.* **1988**, *88*, 322.
(80) van Gisbergen, S. J. A.; Snijders, J. G.; Baerends, E. *J. Comput. Phys. Commun.* **1999**, *118*, 119.
(81) Sheik-Bahae, M.; Said, A. A.; Wei, T.; Hagan, D. J.; van Stryland, E. W. *IEEE J. Quantum Electron.* **1990**, *26*, 760.

***Table 1.*** Cyclic Voltammetric[a] and Optical Data[b] for Complexes **1**−**5** and **1**$^+$−**5**$^+$

| complex ([M]) | $E_{1/2}$ [$i_{pc}/i_{pa}$, $\Delta E_p$] $Ru^{II/III}$ | [M] $\nu_{max}$ [$\epsilon$] | [M]$^+$ $\nu_{max}$ [$\epsilon$] |
|---|---|---|---|
| *trans*-[$RuCl_2(dppe)_2$] (**1**) | 0.60 [0.9, 0.07] | 22 660 [0.04]<br>32 170 [0.6]<br>38 006 [sh,5.7]<br>39 930 [6.1] | 13 800 [0.2]<br>21 100 [0.2], 24 540 [0.2]<br>34 200 [3.6] |
| *trans*-[Ru(C≡CPh)Cl$(dppe)_2$] (**2**) | 0.55 [1, 0.07] | 31 350 [2.3]<br>38 480 [5.0] | 12 040 [1.0]<br>16 980 [0.1], 27 290 [0.7], 29 830 [1.3],<br>35 710 [5.2], 36 510 [5.3], 37 310 [5.3] |
| *trans*-[Ru(4-C≡$CC_6H_4$C≡CPh)Cl$(dppe)_2$] (**3**) | 0.55 [1, 0.06] | 25 760 [3.6]<br>37 880 [sh, 4.5]<br>40 150 [5.0] | 11 160 [2.0]<br>15 560 [0.5]<br>21 180 [sh, 1.5], 22 210 [2.6], 24 020 [1.8],<br>31 050 [sh, 2.3], 33 790 [sh, 3.9],<br>35 580 [5.4], 36 650 [5.5], 37 160 [5.4] |
| *trans*-[Ru$(C≡CPh)_2(dppe)_2$] (**4**) | 0.56 [0.9, 0.07] | 30 310 [8.1]<br>41 160 [12.8] | 8920 [3.6], 10 970 [1.5]<br>16 200 [0.6]<br>24 680 [sh, 1.1], 26 370 [1.8]<br>28 970 [3.2]<br>38 270 [11.4] |
| *trans*-[Ru(C≡CPh)(4-C≡$CC_6H_4$C≡CPh)$(dppe)_2$] (**5**) | 0.56 [1, 0.07] | 25 540 [6.8]<br>32 440 [5.0]<br>33 880 [sh, 4.9]<br>36 750 [5.5]<br>41 010 [8.7] | 8440 [2.9], 10 480 [sh, 0.6]<br>15 960 [0.2]<br>21 120 [sh, 0.8], 22 120 [1.3]<br>29 010 [2.8], 32 260 [3.2]<br>37 660 [5.5] |

[a] $CH_2Cl_2$; Pt auxiliary, Pt working, and Ag/AgCl reference electrodes (ferrocene/ferrocenium couple located at 0.56 V, $\Delta E_p = 0.06$ V); $E_{1/2}$, $\Delta E_p$ in V. [b] $CH_2Cl_2$; $\nu_{max}$ in $cm^{-1}$; [$\epsilon$] in $10^4$ $M^{-1}$ $cm^{-1}$; sh = shoulder.

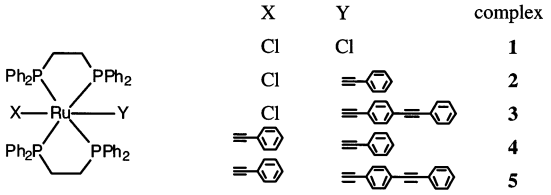


***Figure 1.*** Structural formulas for complexes **1**−**5**.

+3 cm from the focal plane), the beam radius growing by roughly a factor of 10 (i.e., to about 350−450 $\mu$m) over the distance of ten Rayleigh lengths, but still providing for almost complete transmission. The beam transmitted through the electrochemical cell was split in two, one part being focused on an "open aperture" detector, the other part being transmitted through a 1 mm aperture to provide the "closed aperture" signal. *Z*-scans were collected with the electrochemical cell. The electrogeneration potential was 0.8 V to ensure complete electrolysis; this required approximately 5 min. The *Z*-scan measurements were carried out during the electrolysis and were continued while the electrode potential was cycled from 0 to 0.8 V and back to 0 V again. The real and imaginary parts of the nonlinear phase change were determined by numerical fitting using equations given in the literature,[81] assuming that the absorption saturation process can be modeled by a linear dependence of the absorption coefficient on the light intensity.[82] The nonlinearities and light intensities were calibrated using measurements of a 1 mm thick silica plate for which the nonlinear refractive index $n_2 = 3 \times 10^{-16}$ $cm^2$ $W^{-1}$ was assumed.

## Results

**Electrochemical and Spectroelectrochemical Behavior.** The complexes chosen for the present study are displayed in Figure 1. The systematic variation inherent in these complexes permits assessment of the impact of the sequential replacement of chloro by alkynyl ligand (proceeding from **1** to **2** and **4**) and chain lengthening of the alkynyl ligand (proceeding from **2** to **3** and **4** to **5**) on electrochemical and optical properties. The results from cyclic voltammetric studies on complexes **1**−**5** are shown in Table 1. All complexes undergo a reversible to quasi-reversible oxidation assigned to the $Ru^{II/III}$ couple [$i_{pc}/i_{pa} \approx 1$, $\Delta E_p(Ru^{II/III}) \approx \Delta E_p$(ferrocene/ferrocenium)]. In particular, the cyclic voltammograms of these arylalkynyl complexes do not display the features of chemical irreversibility apparent in those of the related thienylalkynyl complexes *trans*-[Ru(C≡C-2-$C_4H_3S)_n(Cl)_{2-n}(dppm)_2$] ($n$ = 1,2),[10] suggesting that complexes **1**−**5** may be more useful for electrochemical switching (see Figure 1).

As we have noted previously, replacement of a chloro ligand by the C≡CPh group in proceeding from *trans*-[$RuCl_2(dppm)_2$] to *trans*-[Ru(C≡CPh)Cl$(dppm)_2$] (**6**) results in a decrease in the $Ru^{II/III}$ oxidation potential.[15,83] In the present series of complexes, replacement of the first chloro ligand of *trans*-[$RuCl_2(dppe)_2$] (**1**) by C≡CPh (to afford **2**) or by the chain-lengthened alkynyl ligand 4-C≡$CC_6H_4$C≡CPh (**3**) results in a slight decrease in the oxidation potential (from 0.60 to 0.55 V), as expected. In contrast, replacement of the chloro ligand in complexes **2** and **3** by an alkynyl ligand to afford the bis-alkynyl complexes **4** and **5** produces no significant change in oxidation potential (from 0.55 to 0.56 V in each case). The results are consistent with those reported previously for complexes **1**,[84] **2**, and **4**.[85] These data suggest that the alkynyl ligands (C≡CPh and 4-C≡$CC_6H_4$C≡CPh) act as slightly better $\sigma$-donor ligands than the chloro ligand, a result consistent with previous studies of *trans*-[Fe(C≡CPh)$_n$(Cl)$_{2-n}$(dmpe)$_2$] [$n$ = 0−2, dmpe = 1,2-bis-(dimethylphosphino)ethane].[86] For the present series of complexes, chain lengthening of the alkynyl ligand (proceeding from **2** to **3** or from **4** to **5**) results in no change in $E_{1/2}$.

(82) Sutherland, R. L., Ed. *Handbook of Nonlinear Optics*; Marcel Dekker: New York, 1996; Vol. 52.

(83) Whittall, I. R.; Cifuentes, M. P.; Humphrey, M. G.; Luther-Davies, B.; Samoc, M.; Houbrechts, S.; Persoons, A.; Heath, G. A.; Bogsanyi, D. *Organometallics* **1997**, *16*, 2631.

(84) Champness, N. R.; Levason, W.; Pletcher, D.; Webster, M. *J. Chem. Soc., Dalton Trans.* **1992**, 3243.

(85) Younus, M.; Long, N. J.; Raithby, P. R.; Lewis, J.; Page, N. A.; White, A. J. P.; Williams, D. J.; Colbert, M. C. B.; Hodge, A. J.; Khan, M. S.; Parker, D. G. *J. Organomet. Chem.* **1999**, *578*, 198.

(86) Field, L. D.; George, A. V.; Laschi, F.; Malouf, E. Y.; Zanello, P. *J. Organomet. Chem.* **1992**, *435*, 347.

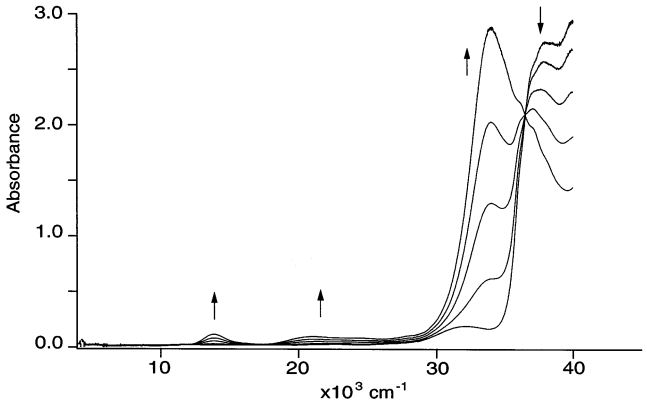


***Figure 2.*** UV−vis−NIR spectral changes during the electrochemical oxidation of *trans*-[$RuCl_2(dppe)_2$] (**1**).

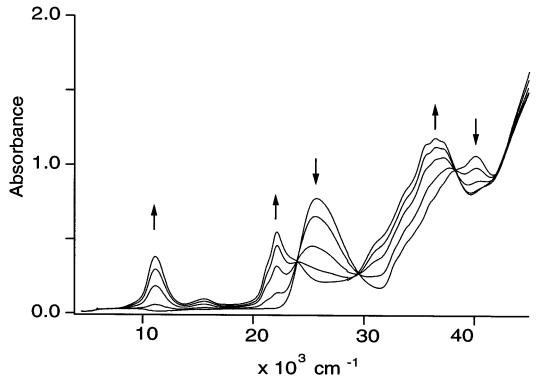


***Figure 3.*** UV−vis−NIR spectral changes during the electrochemical oxidation of *trans*-[$Ru(4\text{-}C{\equiv}CC_6H_4C{\equiv}CPh)Cl(dppe)_2$] (**3**).

UV−vis−NIR absorption data for complexes **1**−**5** are listed in Table 1; the spectra show the expected increase in complexity on proceeding from the dichloro complex (**1**) to the mono- (**2**, **3**) and bis-alkynyl complexes (**4**, **5**). All complexes **1**−**5** are optically transparent at frequencies < 20 000 $cm^{-1}$. The lowest-energy bands in complexes such as **2**−**5** have been tentatively assigned as metal-to-ligand charge transfer in origin,[15,85] but a detailed analysis of the electronic spectra of this class of complex is lacking, and controversy remains: a recent report examining thienylalkynyl complexes *trans*-[$Ru(C{\equiv}CR)Cl(dppm)_2$] and *trans*-[$Ru(C{\equiv}CR)_2(dppm)_2$] (R = 2-$C_4H_3S$, 2,5-$C_4H_2S$-2′-$C_4H_3S$, 2,5-$C_4H_2S$-2′,5′-$C_4H_2S$-2″-$C_4H_3S$) assigned bands in the range 21 740−30 490 $cm^{-1}$ to thiophene-based $\pi-\pi^*$ transitions and localized on each ligand rather than delocalized over the whole complex.[10]

The $Ru^{III}$ complexes $\mathbf{1}^+$−$\mathbf{5}^+$ can be conveniently generated electrochemically in dichloromethane using an OTTLE cell. Oxidation at 253 K using a potential of 0.8 V results in the progressive replacement of spectral peaks because of the starting compound with those of the oxidized species, with isosbestic points in each case. Representative examples of the spectra obtained (those of **1**, **3**, and **5**) are shown in Figures 2−4. The optical spectrum of $\mathbf{1}^+$ as its tetrafluoroborate salt has been reported,[84] the low-energy maximum (13 900 $cm^{-1}$) comparing favorably with that of $\mathbf{1}^+$ as the hexafluorophosphate salt in the present work (13 800 $cm^{-1}$). The earlier report assigned this transition as $\sigma(P) \rightarrow e(Ru)$ charge transfer in nature. The optical spectrum of *trans*-[$Ru\{C{\equiv}CC(=CH_2)NMe_2CH_2Ph\}Cl(dppm_2)]^{2+}$, which contains an ammonium center, has also been examined previously, but no bands lower in energy than 20 000 $cm^{-1}$ were

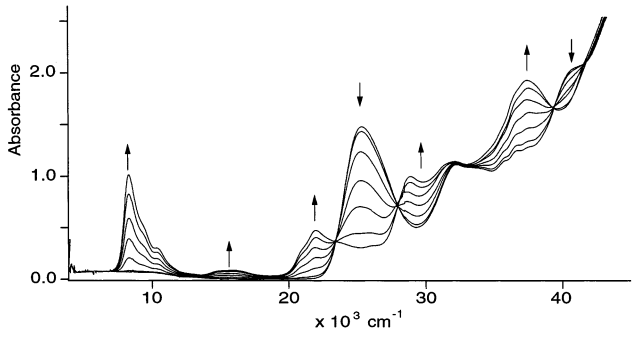


***Figure 4.*** UV−vis−NIR spectral changes during the electrochemical oxidation of *trans*-[$Ru(4\text{-}C{\equiv}CC_6H_4C{\equiv}CPh)(C{\equiv}CPh)(dppe)_2$] (**5**).

reported.[9] The electronic spectra of *trans*-[$Ru(C{\equiv}CR)Cl(dppm)_2]^+$ and *trans*-[$Ru(C{\equiv}CR)_2(dppm)_2]^+$ (R = 2,5-$C_4H_2S$-2′,5′-$C_4H_2S$-2″-$C_4H_3S$) contain bands at 9170 $cm^{-1}$ and 7520 $cm^{-1}$, respectively, assigned (broadly) as LMCT from the terthienyl ligand to Ru(III), although it was not possible to assign these low-energy bands to specific transitions.[10] Similarly, the chemical oxidation of *trans*-[$Ru(4\text{-}C{\equiv}CC_6H_4X)_2(16\text{-TMC})$] (X = OMe, Me, H, F, Cl; 16-TMC = 1,5,9,13-tetramethyl-1,5,9,13-tetraazacyclohexadecane) affords cationic species with optical transitions in the range 13 020−13 970 $cm^{-1}$ assigned as $p_\pi(ArC_2) \rightarrow d_{\pi^*}(Ru^{III})$ LMCT in nature.[11] In the present case, intense NIR bands are seen for the dichloro complex cation ($\mathbf{1}^+$, 13 800 $cm^{-1}$), chloro mono-alkynyl complex cations ($\mathbf{2}^+$, 12 035; $\mathbf{3}^+$ 11 155 $cm^{-1}$), and bis-alkynyl complex cations ($\mathbf{4}^+$, 8920; $\mathbf{5}^+$, 8440 $cm^{-1}$) in a spectral region transparent for the $Ru^{II}$ complexes **1**−**5**. The low-energy transitions for bis-alkynyl complex cations are suggestive of the presence of vibronic progressions, with the $\Delta\nu$ values ($\mathbf{4}^+$, 2050 $cm^{-1}$; $\mathbf{5}^+$, 2040 $cm^{-1}$) consistent with their assignment as $\nu(C{\equiv}C)$ in nature, a result similar to that observed with [$Ru(4\text{-}C{\equiv}CC_6H_4OMe)_2(16\text{-TMC})]^+$.[11] To understand the nature of the electronic transitions in the present series of complexes, calculations employing time-dependent density functional theory were promulgated.

**Computational Results.** Time-dependent density functional theory (TD-DFT) has been used previously to calculate optical transitions in large molecules;[87,88] generally good correlations between experimental and calculated results are obtained, but deviations of up to 8000 $cm^{-1}$ in energies have been reported.[89] In the present case, the coordinate system used in the geometry optimization was maintained for subsequent calculations of optical excitation energies. The calculated frequencies and oscillator strengths from TD-DFT studies are summarized in Tables 2−4, together with assignment of the most important contributions to the optical transitions. The calculations indicate that there is a considerable mixing of Ru d orbitals with alkynyl and/or chloro orbitals for the major transitions. The description of the orbitals involved in the assignments in Tables 3 and 4 can be appreciated from the MO diagrams shown in Figures 5 and 6. Tables 2−4 also contain experimental and calculated frequencies and extinction coefficients/oscillator strengths. The calculated transition energies are generally in good agreement with the experimental results, differences being typically < 4000 $cm^{-1}$; these differences are most likely due to a combination

(87) Ricciardi, G.; Rosa, A.; van Gisbergen, S. J. A.; Baerends, E. J. *J. Phys. Chem. A.* **2000**, *104*, 635.
(88) Geng, L.; Wright, J. C. *Chem. Phys. Lett.* **1996**, *249*, 105.
(89) van Gisbergen, S. J. A.; Groeneveld, J. A.; Rosa, A.; Snijders, J. G.; Baerends, E. J. *J. Phys. Chem. A* **1999**, *103*, 6835.

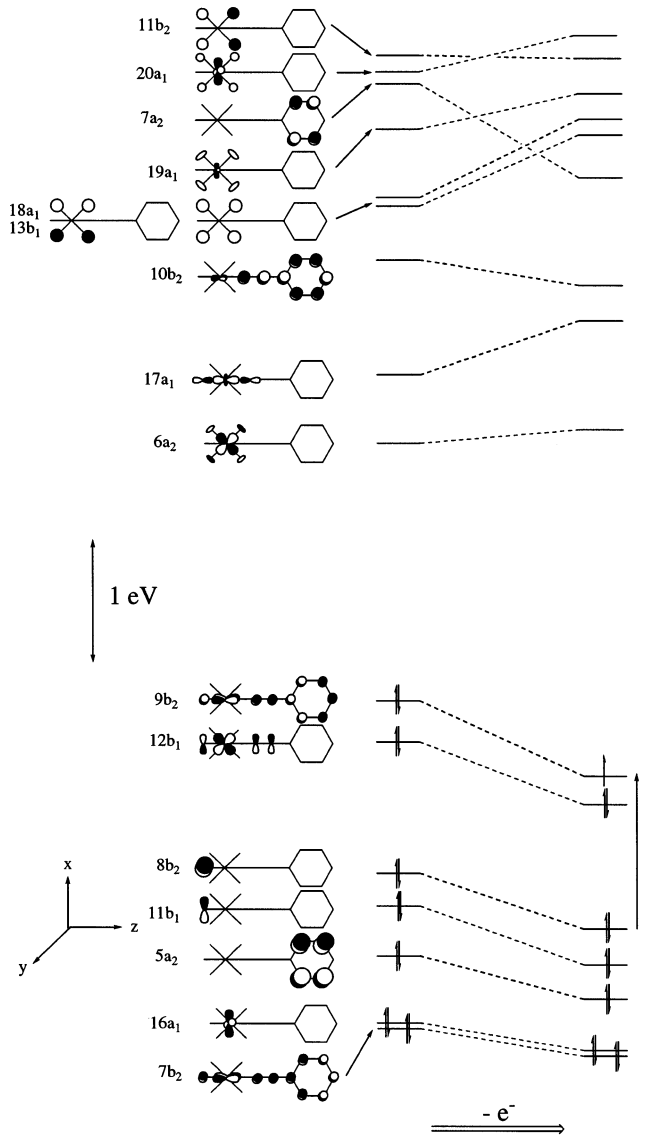


***Figure 5.*** Orbital diagram for *trans*-[Ru(C≡CPh)Cl(PH$_3$)$_4$] showing the effect of oxidation on the energy levels. The arrow indicates the excitation which leads to the strong low-energy band.

***Table 2.*** Calculated Optical Transitions for *trans*-[RuCl$_2$(PH$_3$)$_4$] and Relevant Experimental Data for *trans*-[RuCl$_2$(dppe)$_2$] (**1**)[a]

| 1 | | | |
|---|---|---|---|
| $\nu_{max}$ [$\epsilon$] (expt)[a] | $\nu_{max}$ [$f$] (calcd)[a] | composition | major assignment |
| 22 660 [0.04] | 28 630 [7.3 × 10$^{-4}$] | 10a$_1$ → 11a$_1$ | Cl p$_z$ → Ru d$_{x^2-y^2}$ + Ru d$_{z^2}$ |
| | 29 520 [2.2 × 10$^{-5}$] | 6b$_1$ → 7b$_1$ | Ru d$_{xz}$ + Cl → PH$_3$ |
| 32 170 [0.6] | 30 250 [0.018] | 7b$_2$ → 8b$_2$ | Cl p$_y$ → Ru d$_{yz}$ + PH$_3$ |
| 38 006 [sh, 5.7], 39 939 [6.1] | [b] | | phenyl → phenyl* |

[a] $\nu_{max}$ in cm$^{-1}$; [$\epsilon$] in 10$^4$ M$^{-1}$ cm$^{-1}$. [b] Not applicable.

of vibrational effects, gas phase modeling, and replacement of each dppe by two computationally simpler PH$_3$ ligands. The calculations suggest that the electronic spectra of **2**−**5** contain a metal-to-alkynyl charge-transfer band as the dominant low-energy transition (two in the case of **5**). In all cases, metal-to-phosphorus charge transfer also plays a significant role. In the case of **1**, the intense band at 32 170 cm$^{-1}$ is due to chloro-to-metal charge transfer.

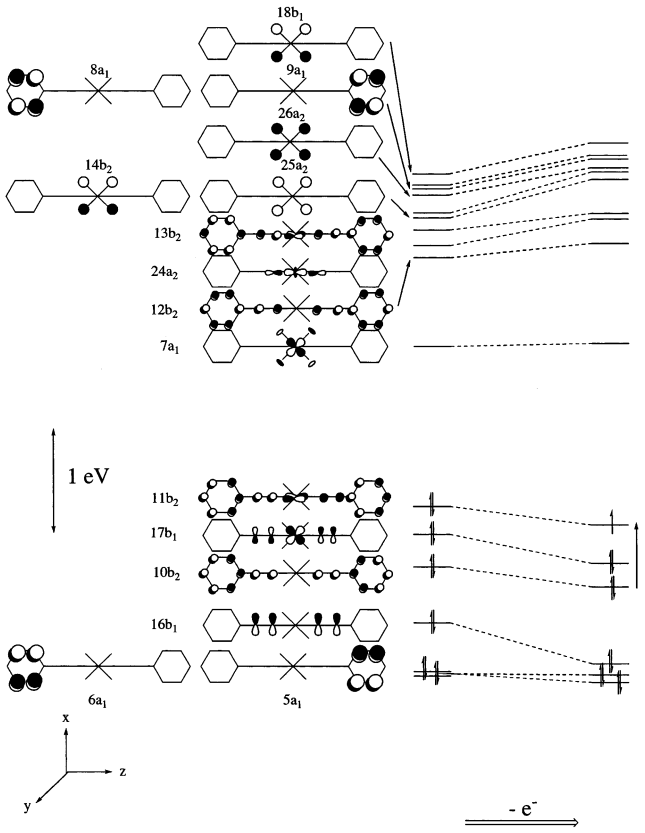


***Figure 6.*** Orbital diagram for *trans*-[Ru(C≡CPh)$_2$(PH$_3$)$_4$] showing the effect of oxidation on the energy levels. The arrow indicates the excitation which leads to the strong low-energy band.

***Table 3.*** Calculated Optical Transitions for *trans*-[Ru(C≡CPh)Cl(PH$_3$)$_4$] and *trans*-[Ru(4-C≡CC$_6$H$_4$C≡CPh)Cl(PH$_3$)$_4$] and Relevant Experimental Data for *trans*-[Ru(C≡CPh)Cl(dppe)$_2$] (**2**) and *trans*-[Ru(4-C≡CC$_6$H$_4$C≡CPh)Cl(dppe)$_2$] (**3**)[a]

| **2** | | | |
|---|---|---|---|
| $\nu_{max}$ [$\epsilon$] (expt) | $\nu_{max}$ [$f$] (calcd) | composition | major assignment |
| 31 350 [2.3] | 29 250 [0.16] | 9b$_2$ → 10b$_2$ | Ru d$_{yz}$ → C$_2$Ph |
| | 29 780 [0.039] | 12b$_1$ → 13b$_1$ | Ru d$_{xz}$ → PH$_3$ |
| | 31 260 [0.18] | 9b$_2$ → 11b$_2$ | Ru d$_{yz}$ → PH$_3$ |
| 38 480 [5.0] | [b] | | phenyl → phenyl* |

| **3** | | | |
|---|---|---|---|
| $\nu_{max}$ [$\epsilon$] (expt) | $\nu_{max}$ [$f$] (calcd) | composition | major assignment[c] |
| 25 760 [3.6] | 21 950 [0.82] | 12b$_2$ → 13b$_2$ | Ru d$_{yz}$ → C$_2$R |
| | 27 690 [0.15] | 12b$_2$ → 14b$_2$ | Ru d$_{yz}$ → PH$_3$ |
| | 28 390 [0.27] | 11b$_2$ → 13b$_2$ | Ru d$_{yz}$ → C$_2$R |
| 37 880 [sh, 4.5] | 30 030 [0.49] | 12b$_2$ → 15b$_2$ | Ru d$_{yz}$ → C$_2$R + PH$_3$ |
| 40 150 [5.0] | [b] | | phenyl → phenyl* |

[a] $\nu_{max}$ in cm$^{-1}$; [$\epsilon$] in 10$^4$ M$^{-1}$ cm$^{-1}$. [b] Not applicable. [c] R = 4-C$_6$H$_4$C≡CPh.

Because of the open-shell nature of the oxidized complexes, the assignment of the low-lying optical transitions in the oxidized complexes has been determined by the ΔSCF method. Since the low-lying transitions are lower in energy than the HOMO−LUMO energy gap, it was assumed that the transition was due to the excitation of an electron from a low-energy level into the "hole" in the HOMO. As all significant absorptions in the complexes **2**−**5** are due to $A_1$ symmetry transitions, it is probable that, for **2**$^+$−**5**$^+$, the transition also has $A_1$ symmetry. Table 5 lists experimental results and calculated energy level

***Table 4.*** Calculated Optical Transitions for *trans*-[Ru(C≡CPh)$_2$(PH$_3$)$_4$] and *trans*-[Ru(4-C≡CC$_6$H$_4$C≡CPh)(C≡CPh)(PH$_3$)$_4$] and Relevant Experimental Data for *trans*-[Ru(C≡CPh)$_2$(dppe)$_2$] (**4**) and *trans*-[Ru(4-C≡CC$_6$H$_4$C≡CPh)(C≡CPh)(dppe)$_2$] (**5**)[a]

**4**

| $\nu_{max}$ [$\epsilon$] (expt) | $\nu_{max}$ [$f$] (calcd) | composition | major assignment |
|---|---|---|---|
| 30 310 [8.1] | 26 050 [0.37] | $11b_2 \rightarrow 12b_2$ | Ru $d_{yz} \rightarrow C_2Ph$ |
| | 26 680 [0.023] | $11b_2 \rightarrow 13b_2$ | Ru $d_{yz} \rightarrow PH_3$ |
| | | $11b_2 \rightarrow 14b_2$ | Ru $d_{yz} \rightarrow PH_3$ |
| | 28 110 [0.091] | $11b_2 \rightarrow 14b_2$ | Ru $d_{yz} \rightarrow PH_3$ |
| | | $10b_2 \rightarrow 12b_2$ | $C_2Ph$ internal |
| | 31 350 [0.061] | $10b_2 \rightarrow 13b_2$ | $C_2Ph \rightarrow PH_3$ |
| | | $10b_2 \rightarrow 14b_2$ | $C_2Ph \rightarrow PH_3$ |
| | 31 750 [0.037] | $17b_1 \rightarrow 18b_1$ | Ru $d_{xz} \rightarrow PH_3$ |
| | 33 360 [0.23] | $10b_2 \rightarrow 12b_2$ | $C_2Ph$ internal |
| | 34 200 [0.24] | $10b_2 \rightarrow 14b_2$ | $C_2Ph \rightarrow PH_3$ |
| 41 160 [12.8] | [b] | | phenyl $\rightarrow$ phenyl* |

**5**

| $\nu_{max}$ [$\epsilon$] (expt) | $\nu_{max}$ [$f$] (calcd) | composition | major assignment |
|---|---|---|---|
| 25 540 [6.8] | 20 130 [0.47] | $14b_2 \rightarrow 15b_2$ | Ru $d_{yz}$ + PhC≡CC$_6$H$_4$C≡CRuC≡CPh $\rightarrow$ C$_2$C$_6$H$_4$C≡CPh |
| | 24 910 [0.81] | $13b_2 \rightarrow 15b_2$ | Ru $d_{yz}$ + PhC≡CC$_6$H$_4$C≡CRuC≡CPh $\rightarrow$ C$_2$C$_6$H$_4$C≡CPh |
| 32 440 [5.0] | 26 490 [0.046] | $14b_2 \rightarrow 16b_2$ | Ru $d_{yz}$ + PhC≡CC$_6$H$_4$C≡CRuC≡CPh $\rightarrow$ $C_2Ph$ |
| 33 880 [4.9] | 27 804 [0.053] | $14b_2 \rightarrow 17b_2$ | Ru $d_{yz}$ + PhC≡CC$_6$H$_4$C≡CRuC≡CPh $\rightarrow$ $PH_3$ |
| 36 750 [5.5] | 29 690 [0.35] | $14b_2 \rightarrow 18b_2$ | Ru $d_{yz}$ + PhC≡CC$_6$H$_4$C≡CRuC≡CPh $\rightarrow$ C$_2$C$_6$H$_4$C≡CPh |
| 41 010 [8.7] | [b] | | phenyl $\rightarrow$ phenyl* |

[a] $\nu_{max}$ in cm$^{-1}$; [$\epsilon$] in 10$^4$ M$^{-1}$ cm$^{-1}$. [b] Not applicable.

***Table 5.*** Calculated Energies of the Low-Energy Transitions for **2**$^+$−**5**$^+$ [a]

| complex | $\nu_{max}$ (expt) | $\epsilon$ (expt) | transition | $\Delta E$ (calcd) | major assignment |
|---|---|---|---|---|---|
| *trans*-[Ru(C≡CPh)Cl(dppe)$_2$]$^+$ (**2**$^+$) | 12 040 | 1.0 | $8b_2 \rightarrow 9b_2$ | 9300 | Cl $p_y \rightarrow$ Ru $d_{yz}$ + $C_2Ph$ |
| | 16 980 | 0.1 | $7b_2 \rightarrow 9b_2$ | 17 400 | Ru $d_{yz}$ + $C_2Ph \rightarrow$ Ru $d_{yz}$ + $C_2Ph$ |
| | | | $6b_2 \rightarrow 9b_2$ | 24 100 | Ru $d_{yz}$ + $C_2Ph \rightarrow$ Ru $d_{yz}$ + $C_2Ph$ |
| *trans*-[Ru(4-C≡CC$_6$H$_4$C≡CPh)Cl(dppe)$_2$]$^+$ (**3**$^+$) | | | $11b_2 \rightarrow 12b_2$ | 7200 | Cl $p_y \rightarrow$ Ru $d_{yz}$ + $C_2$ |
| | 11 160 | 2.0 | $10b_2 \rightarrow 12b_2$ | 11 600 | Cl $p_y$ + Ru $d_{yz} \rightarrow$ Ru $d_{yz}$ + $C_2$ |
| | 15 560 | 0.5 | $9b_2 \rightarrow 12b_2$ | 18 100 | Cl $p_y \rightarrow C_2Ph$ |
| *trans*-[Ru(C≡CPh)$_2$(dppe)$_2$]$^+$ (**4**$^+$) | 8920 | 3.6 | $10b_2 \rightarrow 11b_2$ | 5700 | $C_2Ph \rightarrow$ Ru $d_{yz}$ + $C_2$ |
| | 16 200 | 0.6 | $9b_2 \rightarrow 11b_2$ | 15 800 | Ph $\rightarrow$ Ru $d_{yz}$ + $C_2$ |
| | | | $8b_2 \rightarrow 11b_2$ | 20 000 | $C_2Ph \rightarrow$ Ru $d_{yz}$ + $C_2$ |
| *trans*-[Ru(C≡CPh)(4-C≡CC$_6$H$_4$C≡CPh)(dppe)$_2$]$^+$ (**5**$^+$) | | | $13b_2 \rightarrow 14b_2$ | 4200 | $C_2 \rightarrow$ Ru $d_{yz}$ |
| | 8440 | 2.9 | $12b_2 \rightarrow 14b_2$ | 9600 | $PhC_2C_6H_4C_2 \rightarrow$ Ru $d_{yz}$ + $C_2$ |
| | 15 960 | 0.2 | $11b_2 \rightarrow 14b_2$ | 16 700 | Ru $d_{yz}$ + $C_2Ph \rightarrow$ Ru $d_{yz}$ + $C_2$ |

[a] $\nu_{max}$ in cm$^{-1}$; [$\epsilon$] in × 10$^4$ M$^{-1}$ cm$^{-1}$; $\Delta E$ in cm$^{-1}$.

gaps. As with the neutral complexes, the calculated values correlate well with the experimental results. Some predicted transitions were not observed, presumably because of poor overlap between the relevant orbitals. Figures 5 and 6 contain molecular orbital diagrams for *trans*-[Ru(C≡CPh)X(PH$_3$)$_4$] (X = Cl, C≡CPh). These MO diagrams show that the HOMO−LUMO energy difference for *trans*-[Ru(C≡CPh)Cl(PH$_3$)$_4$] and *trans*-[Ru(C≡CPh)$_2$(PH$_3$)$_4$] are very similar, approximately 2 eV. Likewise, the HOMOs and LUMOs of these two complexes are also very similar in character. The HOMO is delocalized about the Ru $d_{yz}$ and $p_y$ orbitals (the latter from C and Cl in the case of *trans*-[Ru(C≡CPh)Cl(PH$_3$)$_4$]). The LUMO, on the other hand, is mostly Ru $d_{xz}$ in nature, with small amounts of P s orbital character mixed in. Upon oxidation, the frontier orbital gap increases by approximately 30% for *trans*-[Ru(C≡CPh)-Cl(PH$_3$)$_4$], as is apparent from Figure 5. The increase for *trans*-[Ru(C≡CPh)$_2$(PH$_3$)$_4$], however, is much smaller.

**Nonlinear Optical Studies.** The cyclic voltammetry studies revealed that **1**−**5** undergo reversible oxidation in solution, assigned to metal-centered Ru$^{II/III}$ processes, and the UV−vis−NIR spectroelectrochemistry studies showed that these oxidation processes "switched on" optical transitions which have been assigned by TD-DFT calculations. These linear electrochromic effects should also be reflected in modifications of the NLO properties of the molecules. In terms of a sum-over-states description of the optical nonlinearity, any modification of the absorption spectrum of a molecule contributes to the modification of the nonlinear polarizabilities of all orders. The effects are expected to be the most dramatic if the new absorption transitions are in resonance with appropriate combinations of input frequencies.

Relevant data at 800 nm are summarized in Table 6. The dppm-containing analogue of **2**, namely *trans*-[Ru(C≡CPh)Cl-(dppm)$_2$] (**6**), has been utilized here. Differences in optical nonlinearities on replacing bidentate diphosphine are minor and significantly less than errors in data reported in Table 6 [note also that relevant linear optical spectroscopic and electrochemical parameters for these complexes are essentially identical: $\nu_{max}$[$\epsilon$] 31 350 [2.3] (*2*) (Table 3) cf. 31 400 cm$^{-1}$ [2.3 × 10$^{-4}$ M$^{-1}$ cm$^{-1}$] (**6**) (Table 6), $E°$ [$i_{pc}/i_{pa}$] 0.55 [1.0] (**2**)[47] cf. 0.55 V [1.0] (**6**)[15]. Note that in several cases the error of a measurement approaches or equals the magnitude of the value. The critical factor with these measurements is the product of the nonlinearity and solubility; if the contribution of the solute nonlinearity to the total nonlinearity of a solution is less than about 10% (the typical accuracy of a nonlinearity determination), one cannot obtain a precise value from concentration dependence studies in solution. In the present studies, this is not a major concern,

***Table 6.*** Optical Data for Complexes **6**/**6**$^+$, **3**/**3**$^+$, and **5** at 800 nm[a]

| complex | $\nu_{max}$ | $\epsilon$ | $\gamma_{real}$ | $\gamma_{imag}$ | $\lvert\gamma\rvert$ | $\sigma_2$ |
|---|---|---|---|---|---|---|
| *trans*-[Ru(C≡CPh)Cl(dppm)$_2$] (**6**) | 31 400 | 2.3 | <300 | <200 | ≅0 | ≅0 |
| **6**$^+$ | 12 000 | 1.0 | 1300 ± 500 | −2200 ± 1000 | 2600 ± 1000 | −540 ± 200 |
| *trans*-[Ru(4-C≡CC$_6$H$_4$C≡CPh)Cl(dppe)$_2$] (**3**) | 25 800 | 3.6 | −100 ± 100 | 450 ± 200 | 460 ± 200 | 110 ± 50 |
| **3**$^+$ | 11 200 | 2.0 | 2900 ± 1000 | −1200 ± 600 | 3100 ± 1000 | −300 ± 70 |
| *trans*-[Ru(4-C≡CC$_6$H$_4$C≡CPh)(C≡CPh)(dppe)$_2$] (**5**) | 26 100 | 3.8 | −670 ± 300 | 1300 ± 300 | 1500 ± 500 | 310 ± 70 |

[a] $CH_2Cl_2$; $\nu_{max}$ in $cm^{-1}$; [$\epsilon$] in $10^4$ $M^{-1}$ $cm^{-1}$; $\gamma$ in $10^{-36}$ esu, $\sigma_2$ in $10^{-50}$ $cm^4$ s.

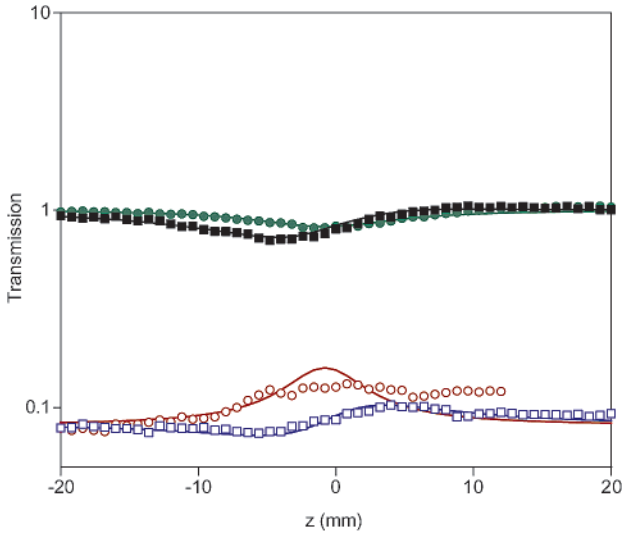


***Figure 7.*** Open (circles) and closed (squares) aperture *Z*-scans for **3** (filled symbols) and **3**$^+$ (open symbols), measured in situ in an electrochemical *Z*-scan cell. Concentration: 0.2%. Note the logarithmic scale of the transmission values

as it is the dramatic increase in the magnitude and change of sign of the nonlinearity which are of interest, and which the experimental data clearly substantiates. In the resting state ($Ru^{II}$ complexes), nonlinearities are low, as expected for these small nondipolar molecules, increasing values being observed on $\pi$-system lengthening (proceeding from **6** to **3** to **5**). Real components $\gamma_{real}$ are negative, and imaginary components $\gamma_{imag}$ and corresponding two-photon absorption cross sections $\sigma_2$ are significant, consistent with observations for related alkynylruthenium complexes.[55,56]

Figure 7 shows an example of the results obtained during the electrochemical switching of **3**. Similar to the results shown by us for 1,3,5-{*trans*-[RuCl(dppe)$_2$]C≡C-4-C$_6$H$_4$C≡C}$_3$C$_6$H$_3$,[47] the electrochemically induced change of transmission (or electrochromic effect) also results in the change of NLO properties of the complex. The characteristic shapes of open and closed aperture scans allow one to provide a simple interpretation of the changes of the optical properties of the molecule. While the neutral molecule **3** is a strong two-photon absorber (as evidenced by a dip in the open aperture scan at zero potential), the oxidized molecule **3**$^+$ has the sign of the absorptive nonlinearity reversed: the maximum in the middle of the scan (distorted by the drift of the background transmission due to the electrochemical reaction still not in equilibrium) is a result of the absorptivity being a decreasing function of the light intensity, which is a characteristic of a saturable absorber.

Thus, the change of sign of the imaginary part of the hyperpolarizability is evident from these results. The changes in the refractive nonlinear properties of the solution are much less self-evident. The shapes of the closed aperture scans are characteristic for a positive total refractive nonlinearity of the system, but this is simply due to the large positive contributions from the solvent and the glass walls of the cell. The numerical fitting and comparison with scans from the cell with those of the electrolyte allow one to calculate the values of the real parts of the hyperpolarizabilities. Table 6 shows these results for **6** and **3** at 800 nm.

Compound **5** is transparent at wavelengths longer than 500 nm, but **5**$^+$ has a strong absorption band centered at 1184 nm and a significant absorption at 1300 nm and was consequently examined in this wavelength range. Results obtained for **5** at longer wavelengths can only be considered preliminary at this stage. Analysis of the results from these measurements indicates that they are influenced to some degree by additional effects which may be due to nonlinearities of nonelectronic origin, possibly of thermal type. Unlike the 800 nm measurements which have been performed with a rather low repetition rate (30 Hz), the laser system for the 1.18−1.3 $\mu$m measurements was operating with a repetition rate of 1 kHz. This, together with the possibility of overtone absorption, may be a factor leading to the effectively negative nonlinearity of the electrochemical cell with the electrolyte solution observed by us. In effect, the nonlinearity due to the **5** and **5**$^+$ solute could not be clearly separated from the background solvent/cell nonlinearity.

## Discussion

The studies summarized earlier have involved identifying compounds with intense reversible electrochromic transitions, which are tunable by appropriate ligand modification and have been assigned by TD-DFT, and utilizing these transitions to switch the signs of $\gamma_{real}$ and $\gamma_{imag}/\sigma_2$ (**3**, **5**) or "switch on" nonlinearities (**6**). The rationale for the latter behavior is straightforward.

Many compounds investigated by us, including **3** and **5** in the present studies, have a strong two-photon absorption effect at 800 nm because of the presence of two-photon accessible states in the vicinity of 400 nm. This is manifested both by a large imaginary part of the cubic hyperpolarizability and by a negative real part of the hyperpolarizability. Dispersion of the hyperpolarizability is likely to lead to a change of sign of the real part of the hyperpolarizability from positive values at longer wavelengths to negative values at wavelengths shorter than that of the two-photon resonance. Since the oxidation of all complexes in the present study introduces long wavelength absorption, its effect is likely to be both a decrease of the two-photon contribution and the introduction of the one-photon resonant contribution if the probing wavelength is in resonance with the new absorption band. Consequently, strong two-photon absorbers such as **3** can have the sign of the components of their third-order nonlinearity at the one-photon absorption frequency reversed on oxidation, while complexes such as **2** and **6** (with low third-order nonlinearity) can have their

nonlinearity "switched on" upon oxidation. This is shown clearly by the results of third-order nonlinearities of **6** and **3** determined by the *Z*-scan technique at 800 nm, summarized in Table 6.

Organic compounds have dominated recent studies of molecular materials with potential photonics applications; they are available at comparatively low cost, in high yield by facile syntheses and can have high nonlinearities and desirable materials processing properties. Organometallic complexes have been intensively studied for 15 years but are yet to truly present a viable and justifiable alternative to organic compounds. The studies detailed herein have involved an NLO effect for which organometallic complexes could be superior to organic compounds; fully reversible metal-centered redox processes render organometallic complexes potentially more useful than organic compounds in applications which require more than one oxidation state. The accessibility of differing oxidation states for organometallic complexes such as those studied herein, and consequent strong linear and nonlinear electrochromic properties, promise switchable photonic materials at wavelengths tunable by appropriate ligand modification.

**Acknowledgment.** We thank the Australian Research Council for financial support and Johnson-Matthey Technology Centre for the loan of ruthenium salts (M.G.H.). M.G.H. is an ARC Australian Senior Research Fellow, and M.P.C. is an ARC Australian Research Fellow.

JA0277125